THE
EMBO
JOURNAL

β-Tubulin mutations that cause severe neuropathies disrupt axonal transport

Shinsuke Niwa[1,3], Hironori Takahashi[1,3] and Nobutaka Hirokawa[1,2],*

[1]Department of Cell Biology, Graduate School of Medicine, The University of Tokyo, Tokyo, Japan and [2]Center of Excellence in Genome Medicine Research, King Abdulaziz University, Jeddah, Saudi Arabia

Microtubules are fundamental to neuronal morphogenesis and function. Mutations in tubulin, the major constituent of microtubules, result in neuronal diseases. Here, we have analysed β-tubulin mutations that cause neuronal diseases and we have identified mutations that strongly inhibit axonal transport of vesicles and mitochondria. These mutations are in the H12 helix of β-tubulin and change the negative charge on the surface of the microtubule. This surface is the interface between microtubules and kinesin superfamily motor proteins (KIF). The binding of axonal transport KIFs to microtubules is dominantly negatively disrupted by these mutations, which alters the localization of KIFs in neurons and inhibits axon elongation in vivo. In humans, these mutations induce broad neurological symptoms, such as loss of axons in the central nervous system and peripheral neuropathy. Thus, our data identified the critical region of β-tubulin required for axonal transport and suggest a molecular mechanism for human neuronal diseases caused by tubulin mutations.

Introduction

The distinctive morphology of neurons is supported by the specific microtubule networks that develop in neurons (Hirokawa, 1982; Cleveland, 1987). Kinesin superfamily proteins (KIFs) are microtubule-dependent molecular motors that transport vesicular organelles in axons (Verhey and Hammond, 2009; Hirokawa *et al*, 2010). Microtubules are composed of α- and β-tubulin heterodimers (Mohri, 1968). There are six major classes of β-tubulin in mammals. Three classes of β-tubulin, Class I (TUBB1), Class II (TUBB2) and Class III (TUBB3) are strongly expressed in neurons (Sullivan and Cleveland, 1986; Cleveland, 1987; Joshi and Cleveland, 1989). Of them, TUBB3 is a neuron-specific isoform (Cleveland, 1987; Joshi and Cleveland, 1989). As microtubules are fundamental to the morphology of

neurons, defects in tubulin genes are likely to cause neuronal diseases (Jaglin *et al*, 2009; Poirier *et al*, 2010; Tischfield *et al*, 2010). To date, mutations in β-tubulin genes have been found to cause three different classes of neuronal disease: polymicrogyria, congenital fibrosis of extraocular muscle type 3 (CFEOM3) and malformation of cortical development (MCD). In addition to the specific symptoms of these conditions, the TUBB3 mutations, E410K, D417H and D417N, induce very severe neurological symptoms, such as peripheral neuropathy and loss of axons in many kinds of brain neurons (Tischfield *et al*, 2010). Because microtubules modulate the functions of a variety of proteins, such as molecular motors and microtubule-associated proteins (MAPs), it is speculated that β-tubulin mutations induce a variety of symptoms. However, previous analyses have relied on yeast cells expressing tubulin mutants or fibroblasts derived from patients. As these studies have not performed cell biological analysis in neurons, the molecular mechanisms of these neuronal defects remain largely elusive. In the present study, we identified β-tubulin mutations that significantly inhibit KIF-mediated axonal transport of vesicles and mitochondria through analysis of β-tubulin mutations that induce neurological symptoms. Furthermore, we found that these mutant tubulins inhibit the binding of axonal transport KIFs to microtubules in a dominant-negative fashion, and disrupt the localization of KIFs in hippocampal neurons.

Results

Identification of β-tubulin mutations that affect vesicular axonal transport

We tested whether axonal transport is affected by β-tubulin mutations that cause three different neuronal diseases. Fourteen β-tubulin mutants were tested: TUBB2(S172P), TUBB2(I210T), TUBB2(L228P) and TUBB2(T312M), which cause polymicrogyria; TUBB3(R62Q), TUBB3(R262C), TUBB3(R380C), TUBB3(E410K) and TUBB3(D417H), which cause CFEOM3; and TUBB3(G82R), TUBB3(T178M), TUBB3(A302V), TUBB3(M323V) and TUBB3(M388V), which cause MCD (Jaglin *et al*, 2009; Poirier *et al*, 2010; Tischfield *et al*, 2010). These TUBB2 and TUBB3 mutants were made by PCR-based mutagenesis and fused with a FLAG tag. The TUBB2(S172P) and TUBB2(T312M) mutants were cytoplasmic, and the TUBB2(L228P) mutant was partially incorporated into microtubules. Wild-type TUBB2 and TUBB3 and the other tubulin mutants were incorporated into microtubules in cells (Supplementary Figure S1A), consistent with previous studies (Jaglin *et al*, 2009; Poirier *et al*, 2010; Tischfield *et al*, 2010). These mutations are autosomal dominant (Poirier *et al*, 2010; Tischfield *et al*, 2010); therefore, we hypothesized that ectopic expression should result in some physiological effects. Thus, these tubulin mutants were co-transfected with axonal transport markers into hippocampal neurons. When the improved

Ca^{2+}-phosphate method was performed (Jiang and Chen, 2006), all green fluorescent protein (GFP)-positive neurons were FLAG positive (Supplementary Figure S1B; >50 neurons from five independent transfections for each tubulin mutant were analysed).

In mature hippocampal neurons, VAMP2, an axonal plasma membrane protein, is processed by the Golgi apparatus and is directly sorted into axons; thus, it is widely used as a marker for vesicular axonal transport (Song *et al*, 2009).

Indeed, GFP-VAMP2 specifically accumulated in axons when hippocampal neurons at 10 days *in vitro* (div) were co-transfected with WT-TUBB3 (Figure 1A left panel, and Supplementary Movie S1). Strong signals were observed in axons (Figure 1A, +WT, arrows), while signals in dendrites were relatively weak (Figure 1A, +WT, arrowheads). Among the 14 mutant β-tubulins screened in this study, we found that two TUBB3 mutants, TUBB3(E410K) and TUBB3(D417H), affected the axon-specific localization of
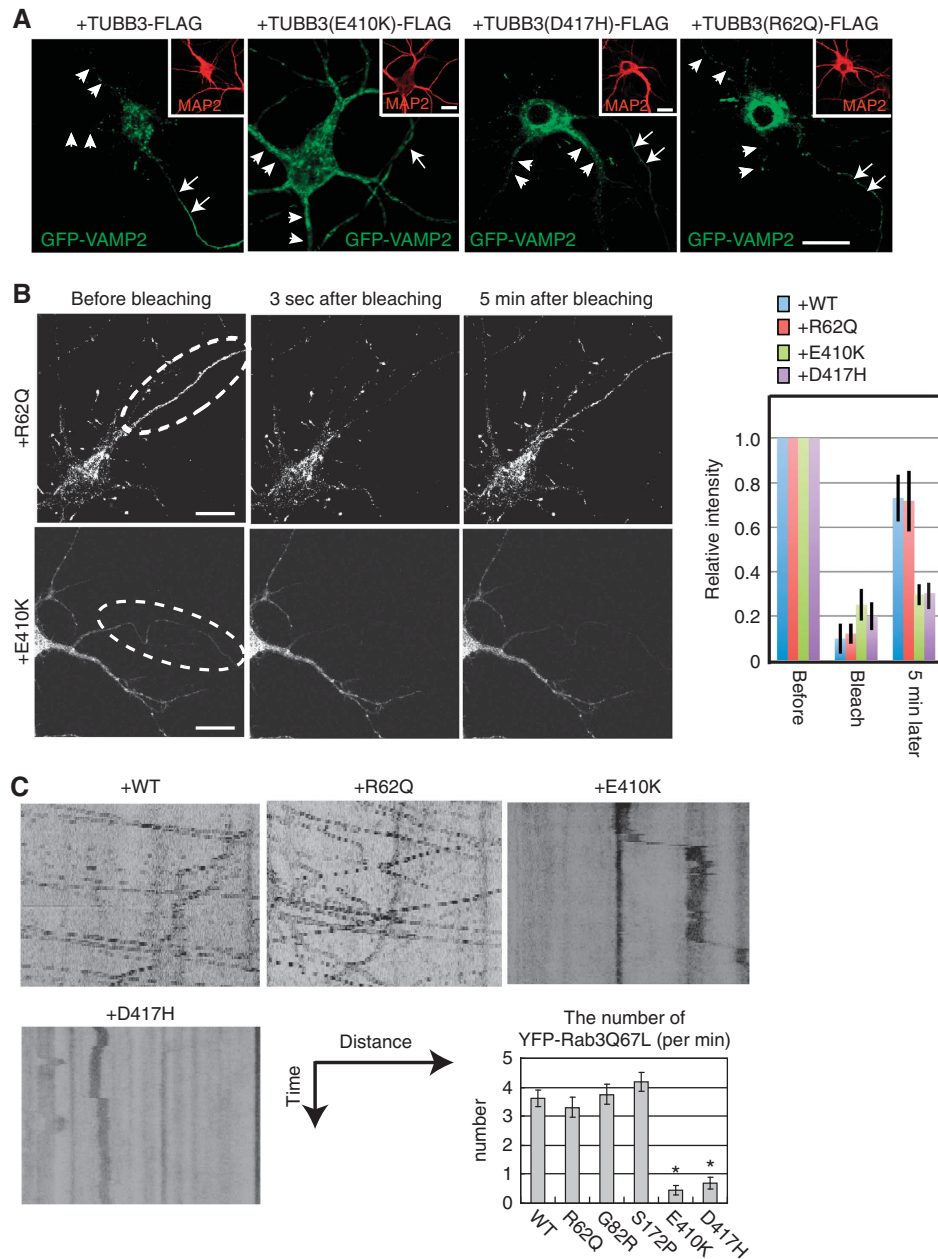

Figure 1 Effect of tubulin mutants on the axonal transport of VAMP2. (**A**, **B**) GFP-VAMP2 vector was co-transfected with FLAG-tagged β-tubulin mutant vectors into 10 div hippocampal neurons, and observed 24 h after transfection. (**A**) Cells were fixed and stained with anti-MAP2 antibody. Representative images of the localization of GFP-VAMP2 (green) and MAP2 (red) in TUBB3, TUBB3(E410K), TUBB3(D417H) and TUBB3(R62Q) mutant-expressing neurons. Arrows and arrowheads indicate MAP2-negative axons and MAP2-positive dendrites, respectively. Bar, 20 μm. (**B**) Representative images of the fluorescence recovery after photobleaching (FRAP) experiments. Images from TUBB3(R62Q)- and TUBB3(E410K)-expressing neurons are shown. Circular areas were photobleached with an argon laser for 1 min to suppress the axonal signals, and time-lapse observation was performed. Bars, 20 μm. Graph shows the quantification of FRAP experiments in WT (Blue), R62Q (Red), E410K (Green) and D417H (Purple). Data are presented as means ± s.d. *P<0.01, *t*-test, compared with WT cells, n = 10. (**C**) YFP-Rab3A(Q81L), a transported form of Rab3 fused with YFP, was co-transfected with β-tubulin mutants into hippocampal neurons at 10 div, and after 24 h, live-cell imaging was conducted. The distance and the time scales represent 50 μm and 100 s, respectively. Sixteen neurons from three independent transfections were counted and are presented graphically. Data are presented as means ± s.e.m. *P<0.01, *t*-test, compared with WT cells, n = 16.

GFP-VAMP2 (Figure 1A; Supplementary Figure S1C). The other mutants did not affect the localization of GFP-VAMP2. In TUBB3(E410K)- and TUBB3(D417H)-expressing cells, the amount of GFP-VAMP2 mis-sorted to dendrites (Figure 1A, central panels, arrow heads) was increased and the polarized localization of GFP-VAMP2 was diminished. Other TUBB3 mutants, such as TUBB3(R62Q), did not change the axon-specific localization of GFP-VAMP2 (Figure 1A, right panel, arrows). Furthermore, fluorescence recovery after photobleaching analysis was performed to investigate any effect on the dynamics of GFP-VAMP2 vesicles. Dynamic motility of vesicle movement was observed in wild-type TUBB3- and TUBB3(R62Q)-expressing cells but not in TUBB3(E410K)- and TUBB3(D417H)-expressing cells. As a result, fluorescent signals were not recovered in TUBB3 (E410K)- and TUBB3(D417H)-expressing axons after 5 min observation (Figure 1B; Supplementary Movies S1 and S2). Statistical analysis using 10 observations supported these observations (Figure 1B, graph). Next, we observed the axonal transport of Rab3A, a synaptic vesicle-associated small GTPase. We have shown that Rab3A is transported by KIF1A and KIF1Bβ in the GTP form. Rab3A with a Q81L mutation is able to mimic the GTP form of Rab3A (Niwa *et al*, 2008). Thus, we used YFP-Rab3A(Q81L) as a probe for the transported form of Rab3A to monitor the axonal transport of Rab3A in mature hippocampal neurons. Similar to the results for GFP-VAMP2 vesicles, the axonal transport of Rab3A was significantly inhibited by co-transfection of TUBB3(E410K) and TUBB3(D417H) mutants (Figure 1C; Supplementary Movie S3). In contrast, co-expression of the other mutants had no effect on the axonal transport of Rab3-carrying vesicles. The number of vesicles anterogradely moving in axons was counted. It was found that the number of Rab3-carrying vesicles transported in axons was significantly reduced in TUBB3(E410K)- and TUBB3(D417H)-expressing neurons but not in TUBB3(R62Q)-, TUBB3(G82R)- and TUBB2(S172P)-expressing neurons (Figure 1C, graph). Although we tried to calculate other parameters such as run length, the number of changes of direction and the average speed, only a very few moving vesicles were observed in TUBB3(E410K)- and TUBB3(D417H)-expressing neurons; thus, we could not observe a sufficient number of moving vesicles. These results indicate that the axonal transport of vesicles is significantly affected by TUBB3 E410K and D417H mutations but not by the other mutations.

TUBB3(E410K) and TUBB3(D417H) mutants affect the axonal transport of mitochondria in peripheral neurons

Interestingly, E410K and D417H mutations in the TUBB3 gene cause peripheral neuropathies but other tubulin mutations do not (Jaglin *et al*, 2009; Poirier *et al*, 2010; Tischfield *et al*, 2010). Several genetic studies have shown that defective axonal transport and impaired mitochondrial functions are causes of peripheral neuropathy (Delettre *et al*, 2000; Zhao *et al*, 2001; Züchner *et al*, 2004; Rivière *et al*, 2011). Thus, we tested the axonal transport of mitochondria in β-tubulin mutant-expressing peripheral neurons using dorsal root ganglion (DRG) neurons, a well-established model of peripheral neurons. To observe the effect of tubulin mutations on mitochondrial transport, a GFP variant fused with a mitochondrial signal derived from cytochrome oxidase IV (GFP-mit) (Llopis *et al*, 1998) was co-transfected with

β-tubulin mutants into DRG neurons using electroporation. Three days after electroporation, DRG cells were observed by time-lapse confocal microscopy. The number of mitochondria moving in cells was significantly reduced in either TUBB3(E410K)- or TUBB3(D417H)-expressing neurons, compared with TUBB3(WT)-expressing neurons (Figure 2A; Supplementary Movie S4). As is the case in vesicle motility (Figure 1), the most obvious effect was reduction in number of moving mitochondria; it was difficult to compare various motility parameters such as run length and changes of moving direction. To exclude a possibility that the expression of GFP-mit affected the axonal transport of mitochondria, we observed the localization of endogenous mitochondria in these cells. For that purpose, wild-type TUBB3- and TUBB3(D417H) mutant-expressing cells were stained with MitoTracker red and fixed. The expression of wild-type TUBB3 and TUBB3(D417H) was monitored by counterstaining with anti-FLAG antibody. Consistent with the live-cell imaging of mitochondrial transport, the number of mitochondria in axons of TUBB3(D417H)-expressing cells was reduced compared with that in control neurons (Figure 2B). Taken together, these data suggest that axonal transport of mitochondria was also affected by expression of the TUBB3(E410K) and TUBB3(D417H) mutants.

Ectopic expression of TUBB3(E410K) and TUBB3(D417H) mutants perturbs the binding of KIFs to microtubules

VAMP2 is transported by KIF5 (Song *et al*, 2009), and Rab3A is transported by KIF1A and KIF1Bβ (Niwa *et al*, 2008), while mitochondria are cargos of KIF5 and KIF1Bα (Nangaku *et al*, 1994; Tanaka *et al*, 1998). We hypothesized that the defective axonal transport of vesicles and mitochondria observed in TUBB3(E410K)- and TUBB3(D417H)-expressing neurons was caused by the inhibition of KIFs. To test this possibility, the binding of KIFs to microtubules was analysed by a microtubule co-sedimentation assay (Bulinski and Borisy, 1979). As a very high transfection efficiency is required for this experiment, 293FT cells, which is sensitive to transfection and can express high amount of proteins, were used. Cells transfected with TUBB2 and TUBB3 mutants and microtubules were then polymerized from transfected cell lysates. Then, 5 mM adenosine 5′-(β,γ-imido) triphosphate (AMP-PNP) and 10 μM taxol were added to lysates, and microtubule and supernatant fractions were separated by ultracentrifugation and analysed by western blotting. While most endogenous KIF5 was bound to microtubules in control cells in the presence of AMP-PNP, a significant amount of KIF5 was detected in the cytoplasmic fraction in TUBB3(E410K)- and TUBB3(D417H)-expressing cell lysates (Figure 3A). The binding of dynein to microtubules was not changed by tubulin mutants. We could not detect the binding of endogenous KIF1Bβ to microtubules even in the presence of AMP-PNP (Figure 3B, upper panels). When brain lysate was analysed by the same assay, similar results were obtained. While endogenous KIF5 bound strongly to microtubules in the presence of AMP-PNP, endogenous KIF1Bβ did not (Figure 3B, lower panels). The tail-inhibition mechanism may affect the binding of KIF1Bβ to microtubules under these conditions (Verhey and Hammond, 2009). Hence, we assayed tail-less KIFs that are free from tail inhibition and are constitutively active (Huang and Banker, 2011). To this end, the motor domains of KIF5(K560), KIF1A(C381),
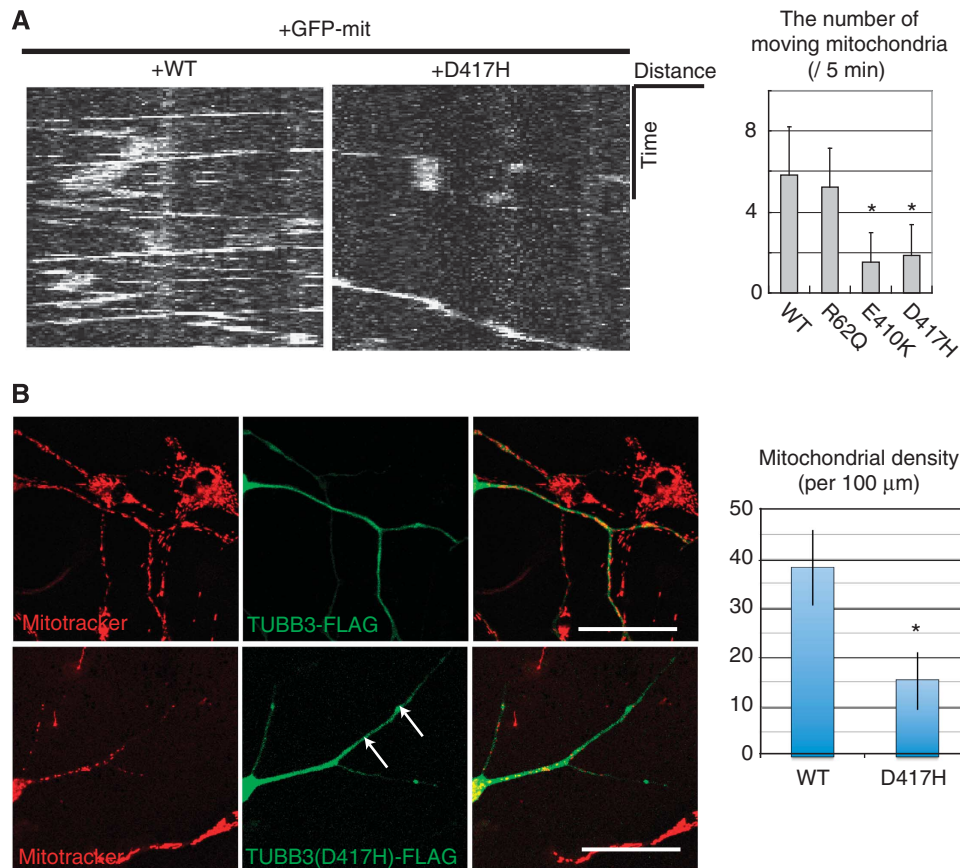
Figure 2 Effect of tubulin mutants on the axonal transport of mitochondria. (**A**) EGFP fused with the mitochondrial localization signal derived from cytochrome oxidase IV (GFP-mit) was co-transfected with β-tubulin-mutant vectors into DRG neurons by electroporation and incubated for 3 days, and live-cell imaging was performed. As examples, kymographs indicating the mitochondrial motility of wild-type TUBB3 and TUBB3(D417H)-expressing neurons are shown. The distance and the time scales represent 50 μm and 10 min, respectively. The graph shows the results of quantification from wild-type TUBB3, TUBB3(R62Q)-, TUBB3(E410K)- and TUBB3(D417H)-mutant expressing cells. The number of anterogradely moving mitochondria passing at a point in axons was counted for 5 min and plotted. Data are presented as means ± s.d. *$P < 0.01$, *t*-test, compared with WT cells. Ten axons from ten neurons that were obtained from three independent transfections were counted. (**B**) Mislocalization of mitochondria in TUBB3(D417H)-expressing DRG neurons. To observe mitochondria, cells were transfected with FLAG-wild-type TUBB3 or FLAG-TUBB3(D417H) vectors, stained with MitoTracker red (Red), fixed and stained with anti-FLAG antibody (Green). Representative images are shown. Bars, 50 μm. Graph shows the mitochondrial density in axons. The number of mitochondria in axons was counted and shown as the number of mitochondria per 100 μm. Data are presented as means ± s.d. *$P < 0.01$, *t*-test, compared with WT cells. Ten axons from ten neurons that were obtained from three independent transfections were counted.

KIF1B(KIF1B470) and KIF21A(KIF21A420) were fused with GFP, co-transfected with tubulin mutants and the binding to microtubules in the presence of AMP-PNP was analysed as described above. As a result, the amount of these motors released from microtubule fractions was significantly augmented by overexpression of TUBB3(E410K) and TUBB3(D417H) (Figure 3C).

Expression of TUBB3(E410K) and TUBB3(D417H) mutants alters the accumulation of KIFs in axonal tips of hippocampal neurons

Previous studies have shown that GFP-K560 specifically accumulates in axonal tips in developing and mature neurons (Nakata and Hirokawa, 2003; Jacobson *et al*, 2006). Therefore, to confirm that expression of TUBB3(E410K) and TUBB3(D417H) changed the activity of KIFs in hippocampal neurons, GFP-K560 was co-transfected with β-tubulin mutants by the Ca^{2+}-phosphate method and its localization was observed. TUBB3(E410K) and TUBB3(D417H) significantly inhibited the axon-specific accumulation of GFP-K560, while other tubulin mutants did not (Figure 4A). The GFP signal

became diffuse in TUBB3(E410K)- and TUBB3(D417H)-expressing neurons. Furthermore, three additional KIFs, KIF1A, KIF1B and KIF21A were tested. To this end, the motor domains of GFP-C381, GFP-KIF1B470 and GFP-KIF21A420 were observed. While GFP-KIF21A420 accumulated in axonal tips, GFP-C381 and GFP-KIF1B470 accumulated in both axonal and dendritic tips (Supplementary Figure S2). Similar to the results for K560, the signals for these three motors became diffuse when co-expressed in neurons with TUBB3(E410K) or TUBB3(D417H) mutants, compared with control cells (Figures 4B and 5A). A mutation in the KIF21A motor domain (C28W) has been reported to cause a neuronal disease, CFEOM1 (Yamada *et al*, 2003; Lu *et al*, 2008). In addition, we have shown that a rigor mutation (T90N) perturbs motor activity (Nakata and Hirokawa, 1995). We therefore expressed these motor domain mutants in hippocampal neurons, and indeed, these two mutations changed KIF21A accumulation in axonal tips (Figure 5B). Taken together, these data suggest that mutations of residues E410 and D417 in TUBB3 can broadly change the property of KIFs in neurons and the localization depends on the motor activity in cells.
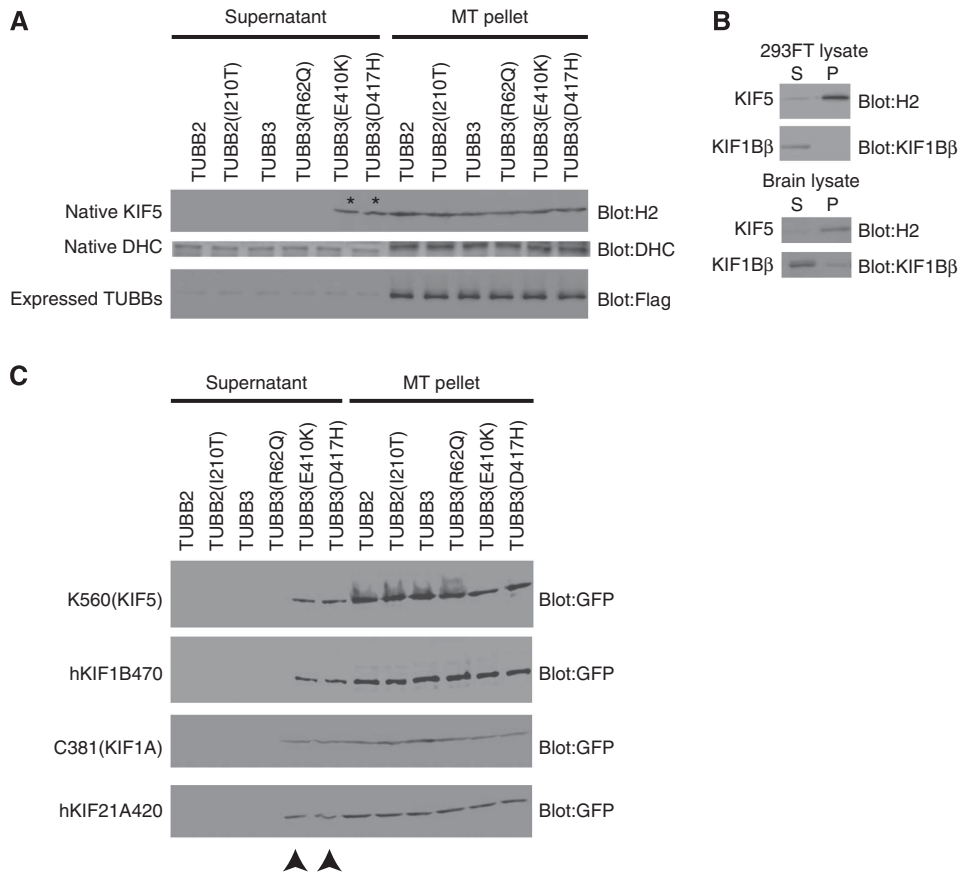
Figure 3 Effects of β-tubulin mutant overexpression on the binding of KIFs to microtubules. (**A**) TUBB2 and TUBB3 mutants were overexpressed in 293FT cells; microtubules were assembled, incubated for 10 min in the presence of 10 μM taxol and 5 mM AMP-PNP and separated by ultracentrifugation. Endogenous KIF5, Dynein and expressed tubulin were detected by the anti-KIF5 antibody (H2), anti-Dynein and the anti-FLAG antibody, respectively. * indicates KIF5 in the supernatant fraction. (**B**) Microtubules were assembled from 293FT cells and mouse brain lysate, incubated for 10 min in the presence of 10 μM taxol and 5 mM AMP-PNP and pelleted by ultracentrifugation. Note that KIF1Bβ does not bind to microtubules under these conditions. (**C**) Tail-less KIF5, KIF1B(hKIF1B470), KIF1A(C381) and KIF21A(hKIF21A420) that were fused with GFP were co-expressed with TUBB2 and TUBB3 mutants in 293FT cells, and analysed as described in (**A**). Arrow heads indicate supernatant fractions containing tail-less KIFs.

The negative charge on the H12 helix is important for axonal transport

E410 and D417 residues are in the H12 helix of TUBB3 and are negatively charged (Figure 6A). The importance of the negative charge on the H12 helix in axonal transport has not been previously analysed. In TUBB3, E421 is also negatively charged, while S413 is on the surface but is not charged (Figure 6A, green and blue, respectively). Thus, TUBB3(E421A) and TUBB3(S413R) were prepared in order to change the negatively charged residue or to give an extra positive charge on the H12 Helix. Furthermore, TUBB3(E410D) and TUBB3(S413A) mutants that do not have altered charges were also prepared as controls. First, these mutant forms of β-tubulin were co-transfected with the motor domain of different KIFs in hippocampal neurons at 2 div and observed in stage 3 neurons. As anticipated, the accumulation of GFP-hKIF21A420 was changed by TUBB3(E421A) and TUBB3(S413R) mutants but not by TUBB3(E410D) or TUBB3(S413A) mutants (Figure 6B). The same results were obtained when GFP-K560, GFP-C381 and GFP-KIF1B470 were investigated (Figure 6B, graph). Thus, β-tubulin mutants that disrupted the surface charge of tubulin changed the localization of GFP-K560, GFP-C381 and GFP-KIF1B370, while β-tubulin mutants that conserved the charge

did not. To show that disruptive motor functions cause the loss of axonal transport, the axonal transport of GFP-VAMP2 was observed in TUBB3(E421A)- and TUBB3(S413R)-expressing neurons. These constructs were co-transfected and observed as described above. As anticipated, expression of these mutant forms of β-tubulin, TUBB3(E421A) and TUBB3(S413R), significantly inhibited the axonal transport of VAMP2-carrying vesicles (Figure 6C; Supplementary Movie S5).

E410K and D417H mutations inhibit axonal transport independent of the tubulin isoform

There are six major β-tubulin families in mammals (Cleveland, 1987; Joshi and Cleveland, 1989). We asked whether the effect of these mutations is TUBB3 specific or is general to β-tubulins. To answer this question, TUBB2(E410K), TUBB2(D417H), TUBB5(E410K) and TUBB5(D417H) mutants were prepared, and their effects on axonal transport of vesicles and the localization of KIFs were observed. All the mutants were incorporated into microtubules in COS-7 cells (Figure 7A). When co-expressed in hippocampal neurons using the Ca^{2+}-phosphate method, all four mutants changed the tip accumulation of GFP-K560 (Figure 7B). Notably, these residues are conserved between
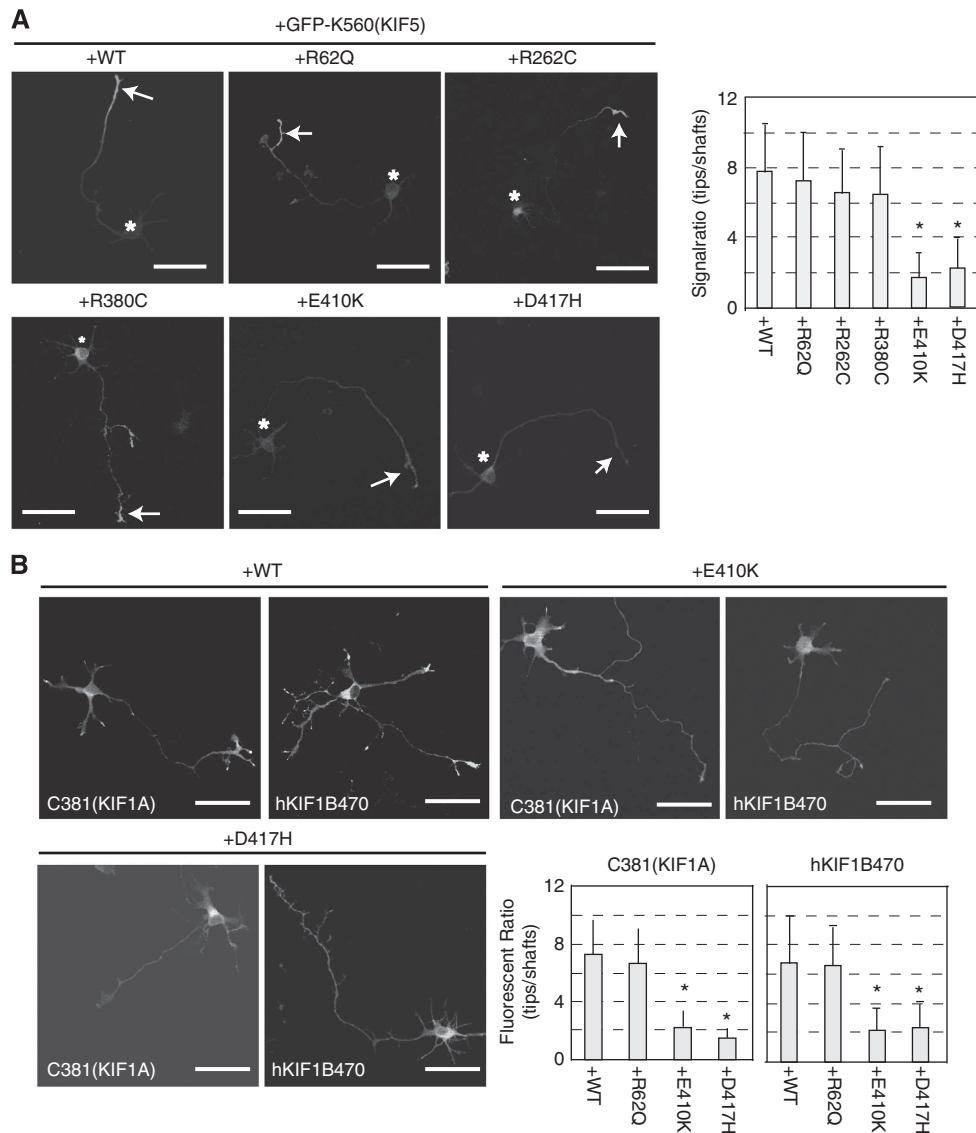
Figure 4 Effects of β-tubulin mutations on the localization of several KIFs. (**A**) The effect of β-tubulin mutations on the localization of the KIF5 motor domain. GFP-K560 vector was co-transfected with FLAG-β-tubulin mutant vectors at 2 div and GFP signals were observed 24 h after transfection. Representative images of the localization of GFP-K560 are shown. Arrows and asterisks, respectively, indicate axons and cell bodies. Bars, 50 μm. Graphs indicate the statistical analysis. Quantification of tip accumulation of GFP-K560 is plotted on the bar graph. Relative intensities were calculated using Equation (1) (Materials and methods). Data are presented as means ± s.d. *$P < 0.01$, Student's *t*-test. Fifteen neurons from three independent transfections were analysed. (**B**) Effect of β-tubulin mutations on the localization of KIF1A and KIF1B motor domains. GFP-C381 or GFP-hKIF1B470 was transfected as in (**A**). Representative images of GFP-C381(KIF1A) or GFP-KIF1B470(KIF1B) in wild-type (WT)-, E410K-β-tubulin- and D417H-β-tubulin-expressing cells. Bars, 50 μm. Graphs indicate the results of quantification. Data are presented as means ± s.d. *$P < 0.01$, Student's *t*-test, 15 neurons from three independent transfections were analysed. Note that E410K and D417H mutants affect the localization of KIF5, KIF1A and KIF1B motor domains.

TUBB genes (Figure 7C). Next, the effect of these mutants on axonal transport was observed. While expression of TUBB2 and TUBB5 did not change the axonal transport of GFP-VAMP2 vesicles, co-expression of TUBB2(E410K), TUBB2(D417H), TUBB5(E410K) and TUBB5(D417H) significantly inhibited transport (Figure 7D; Supplementary Movie S6). Thus, the effects of E410K and D417H mutations are not restricted to the *TUBB3* gene.

Incorporation into microtubules is required to inhibit axonal transport and axonal elongation

TUBB3(E410K) and TUBB3(D417H) mutations are autosomal dominant. Our data indicate that ectopic expression of these

mutants can significantly inhibit axonal transport. As microtubules are polymers composed of α- and β-tubulin dimers, TUBB3(E410K) and TUBB3(D417H) mutants are likely to inhibit axonal transport following incorporation into microtubules. To test this, the S172P mutation was introduced into the TUBB3(E410K) mutant because the S172P mutation completely inhibits β-tubulin incorporation into microtubules (Supplementary Figure S1; Jaglin *et al*, 2009). While TUBB3(E410K) was incorporated into microtubules in COS-7 cells, the double mutated tubulin, TUBB3(S172P, E410K) was not (Figure 8A). First, the effect of these mutants on the localization of GFP-K560 was observed. In TUBB3(E410K)-expressing cells, axonal tip accumulation was
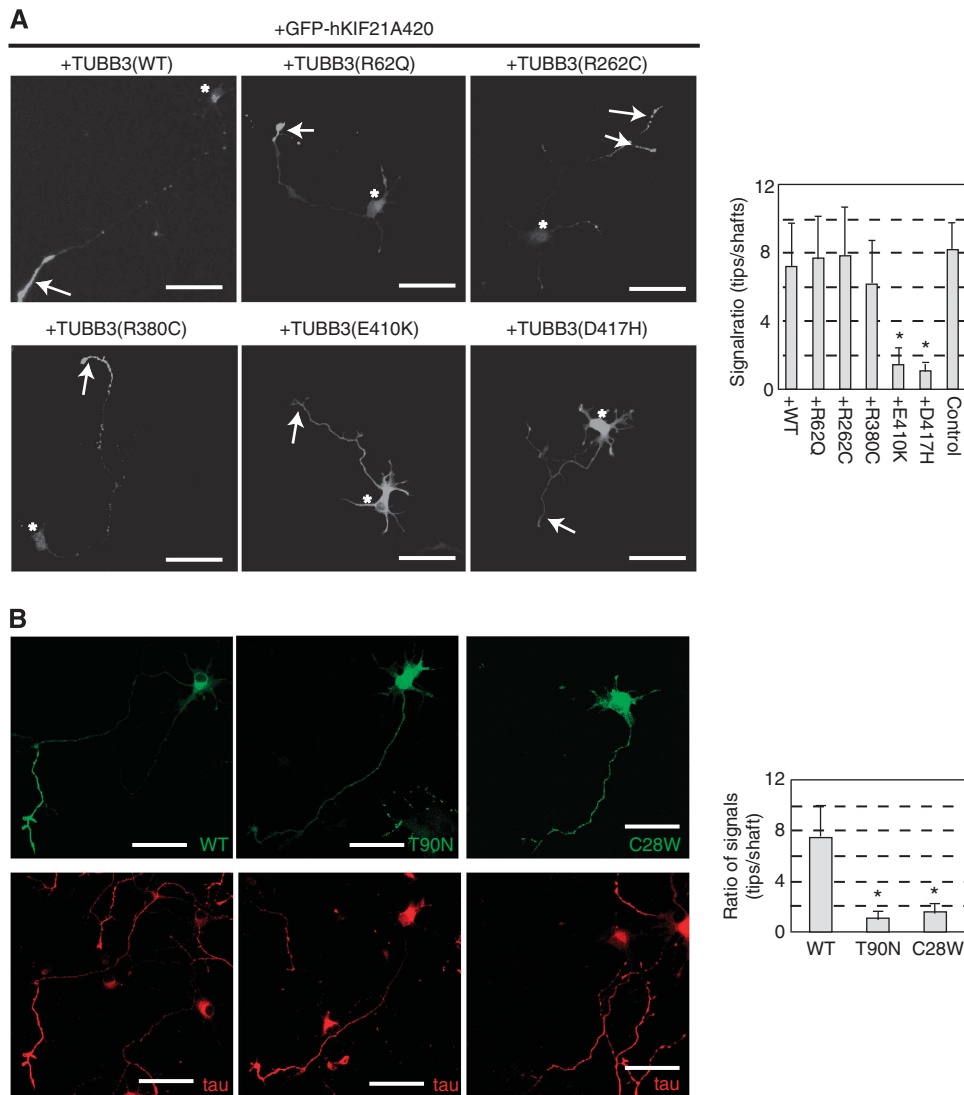
Figure 5 Effects of β-tubulin and motor domain mutations on the localization of KIF21A. (**A**) Hippocampal neurons were co-transfected with GFP-hKIF21A420 and FLAG-β-tubulin mutant vectors and observed at 3 div. Representative images of GFP signals are presented. Arrows and asterisks indicate neurite tips and cell bodies, respectively. Note that co-transfection with E410K and D417H inhibited the tip accumulation of GFP signals. Bar, 50 μm. The graph represents the results of quantification of tip accumulation. Relative intensities were calculated using Equation (1) (Materials and methods). *$P < 0.01$, Student's *t*-test. Data are presented as means ± s.d. Fifteen neurons from three independent transfections were analysed. (**B**) Hippocampal neurons at 2 div were transfected with GFP-hKIF21A420 (green), GFP-hKIF21A420 with the T90N mutation (green) or GFP-hKIF21A420 with the C28W mutation (green), incubated for 24 h and stained by the axon marker, Tau (red). T90N and C28W mutations changed the tip-accumulated localization of GFP-hKIF21A. Bar, 50 μm. Graph indicates quantification of tip accumulation. Relative intensities were calculated using Equation 1 (Materials and methods). Data are presented as means ± s.d. *$P < 0.01$, Student's *t*-test. Sixteen neurons from four independent transfections were analysed.

not observed (Figure 8B, central panel). However, the localization of GFP-K560 in TUBB3(S172P, E410K)-expressing cells was comparable to the localization in control cells (Figure 8B, left panel). Statistical analysis from 20 cells supported these results (Figure 8B, graph). Similarly, the effect of the TUBB3(E410K) mutant on axonal transport of VAMP2 vesicles was reversed by introducing the S172P mutation (Figure 8C; Supplementary Movie S7). Finally, to test the relevance of the cultured neuron data to *in vivo* phenotypes, we performed *in utero* electroporation. WT and mutant TUBB3 were electroporated into 14 day embryonic (E14) mice and observed at postnatal day 1 (P1). When TUBB3 was expressed, tips of axons were elongated and reached the brain midline (Figure 9, TUBB3 WT). In contrast,

tips of axons did not reach the brain midline in TUBB3(E410K) or TUBB3(D417H)-expressing brains (Figure 9, TUBB3 D417H and E410K). To investigate whether or not the incorporation into microtubules is required, the additional S172P mutation, that disrupt the microtubule incorporation, was added to TUBB3(D417H) mutant and the effect was observed. Similarly to the results of cellular experiments (Figure 8), TUBB3(S172P, D417H) did not inhibit axon elongation. To show that disruption of KIFs induces defects of axon elongation, knockdown experiments were performed. An miRNA vector that inhibits the expression of KIF1Bβ (KIF1Bβ-miRNA) was used (Niwa *et al*, 2008) because it has been suggested that KIF1B is required for axon development (Zhao *et al*, 2001). In KIF1Bβ – miRNA
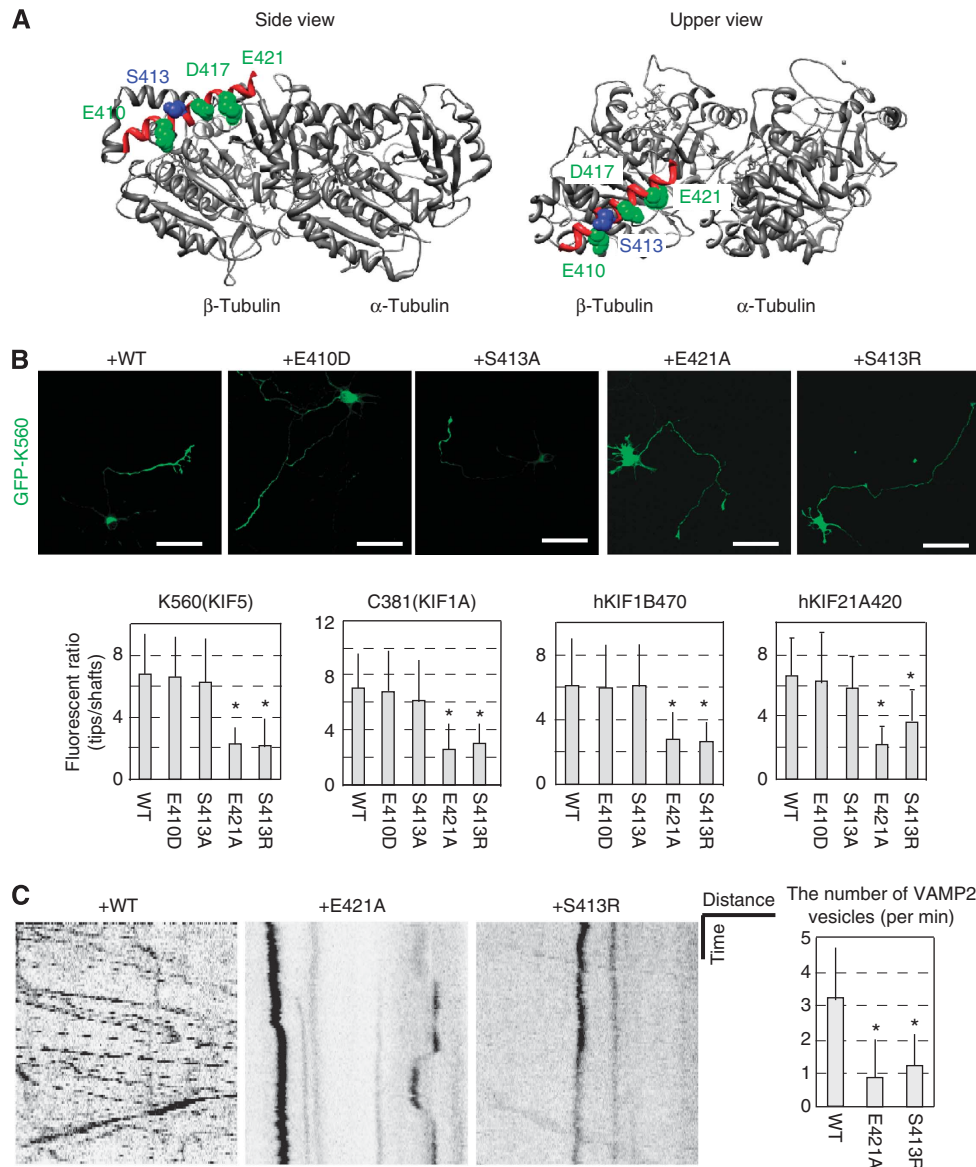
Figure 6 H12 helix supports axonal transport. (**A**) The structure of a tubulin dimer. Data from PDB (#1JFF) were processed using UCSF Chimera software. Side view and upper views are shown. Red indicates the H12 helices of β tubulin. Green indicates negatively charged E410, D417 and E421 residues in the H12 helix. Blue indicates the S413 that is neutral but exposed to the surface. (**B**) Effect of H12 helix mutations on the localization of GFP-K560. One microgram of mutant β-tubulin vectors was co-transfected with 2 μg of GFP-K560, incubated for 24 h and observed at 3 div. Representative images are shown. Bar, 50 μm. Note that E421A and S413R inhibited the accumulation of GFP-K560, while E410D and S413A did not. Graph shows the effects of H12 helix mutations on the localization of KIF5, KIF1A, KIF1B and KIF21A. Hippocampal neurons were observed as described in (**B**). Data are presented as means ± s.d. *$P < 0.01$, Student's *t*-test, 20 neurons from five independent transfections were analysed in each sample. Note that mutations disrupting the negative charges affect the accumulation of all KIFs, while mutations conserving the charge do not. (**C**) GFP-VAMP2 and FLAG-β-tubulin-mutant vectors were co-transfected into hippocampal neurons and incubated for 24 h, and live-cell observation was performed. Kymographs indicate the motility of GFP-VAMP2-carrying vesicles in WT-, TUBB3(E421A)- and TUBB3(S413R)-expressing neurons. The distance and the time scales represent 5 μm and 60 s, respectively. The graph shows the results of quantification. The number of mitochondria moving in axons was counted and plotted. Data are presented as means ± s.d. *$P < 0.01$, *t*-test, compared with WT cells. Ten neurons from three independent transfections were counted.

transfected brains, axon elongation was severely inhibited, compared with that of control miRNA vector-transfected brains.

Discussion

Identification of β-tubulin mutations that strongly inhibit KIF-dependent axonal transport

Mutations in β-tubulin genes cause a broad range of neurological symptoms, such as fibrosis of extraocular muscles, loss of axons in brain neurons, peripheral neuropathy,

polymicrogyria and MCD, depending on the causative mutation (Jaglin *et al*, 2009; Poirier *et al*, 2010; Tischfield *et al*, 2010). There are numerous examples where analysis of hereditary diseases has given insight into the properties of the genes responsible. Analyses of human hereditary neurodegenerative diseases caused by tubulin mutations may yield significant insights into the basic molecular mechanisms of neuronal morphogenesis. Thus, it is thought that analysis of the β-tubulin mutations that cause such neuronal diseases will help the understanding of neuronal morphogenesis. In this work, we have analysed the effects of
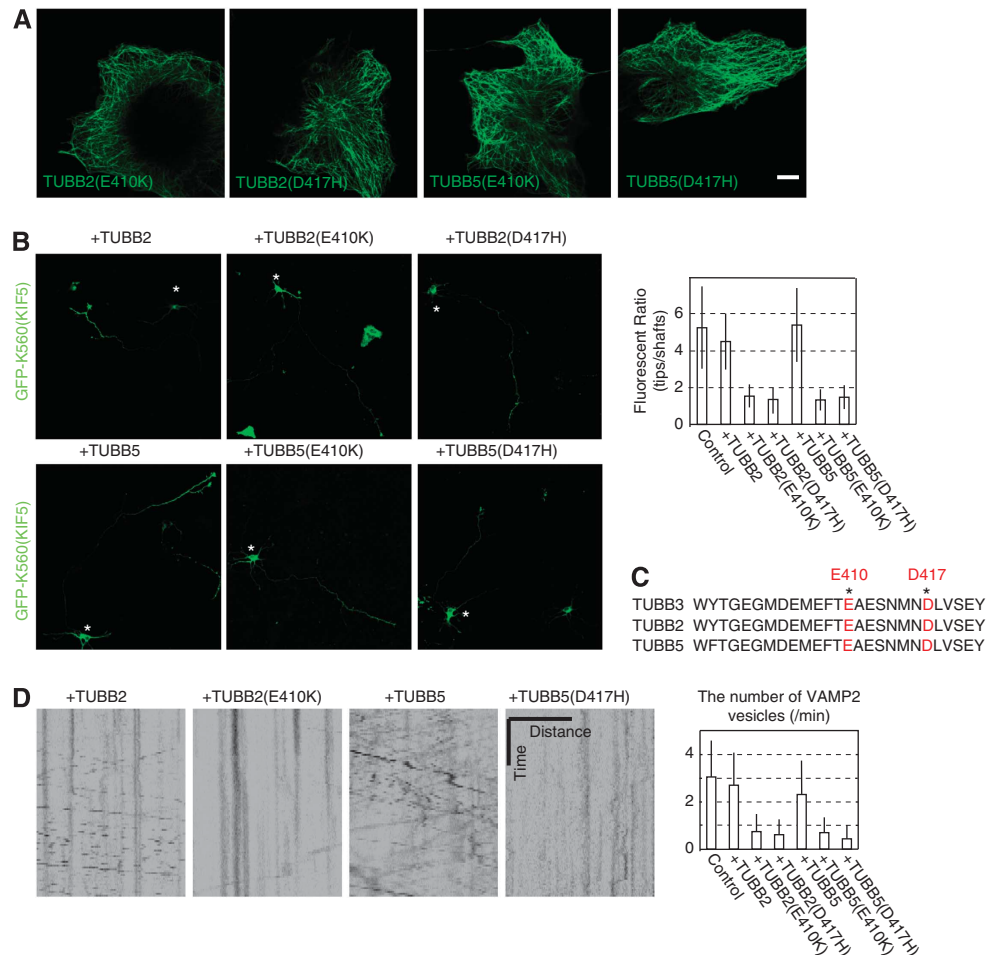
Figure 7 The effect of E410K and D417H mutations is independent of tubulin isoforms. (**A**) TUBB2(E410K), TUBB2(D417), TUBB5(E410K) and TUBB3(D417H) mutants fused with FLAG tag were expressed in COS-7 cells and stained with the anti-FLAG antibody. Bar, 10 μm. (**B**) Effect of E410K and D417H mutations on the localization of GFP-K560. Mutant β-tubulin vectors were co-transfected with GFP-K560 vector, incubated for 24 h and observed at 3 div. Representative images are shown. Bar, 50 μm. Graph shows the effects of E410K and D417H mutations on the localization of GFP-K560. Data are presented as means ± s.d. *P < 0.01, Student's *t*-test. Twenty-four neurons from five independent transfections were analysed for each sample. (**C**) E410 and D417 residues are conserved between β-tubulin isoforms. (**D**) GFP-VAMP2 and FLAG-β-tubulin-mutant vectors were co-transfected into hippocampal neurons and incubated for 24 h, and live-cell observation was performed. Kymographs indicate the motility of GFP-VAMP2-carrying vesicles in TUBB2-, TUBB2(410K)-, TUBB5- and TUBB5(D417H)-expressing neurons. The distance and the time scales represent 10 μm and 60 s, respectively. The graph shows the results of quantification. The number of GFP-VAMP2 vesicles moving in axons was counted and plotted. Data are presented as means + s.d. *P < 0.01, *t*-test, compared with WT cells. Sixteen neurons from three independent transfections were counted.

these mutations in neurons by focusing on axonal transport, which is fundamental to neuronal function and morphogenesis (Hirokawa *et al*, 2010). Through analysing the tubulin mutations that cause neuronal diseases, we found that two mutations, E410K and D417H, perturb axonal transport of vesicles and mitochondria in central and peripheral nervous systems. In the live-cell imaging, the most obvious effect of these mutants is that they reduce the number of moving vesicles (Figures 1 and 2). It suggests that loss of vesicle attachment is the main cause of loss of transport. This is supported by the biochemical data showing that the binding of KIFs is changed by these TUBB3 mutants (Figure 3). Dynein was not affected in biochemical experiments, probably because the binding mechanism is different from KIFs. Nevertheless, retrograde transport was also reduced by these mutant tubulins. It would be the secondary effect of reduction in anterograde transport that supplies cargos to the distal axons. Interestingly, among the β-tubulin

mutants that cause neuronal diseases, E410K and D417H mutations share similar characteristics. They cause broad and severe neurological symptoms, such as peripheral neuropathy and loss of axons in the brain, while other β-tubulin mutations cause relatively mild and more specific symptoms (Jaglin *et al*, 2009; Poirier *et al*, 2010; Tischfield *et al*, 2010). Both E410K and D417H mutations are in the H12 helix of β-tubulin and both mutated residues are negatively charged, suggesting that negative charges on H12 helix are important for axonal transport. Consistent with this idea, the E421 residue, which is also in the H12 helix, is also required for axonal transport (Figure 6). Furthermore, the S413R mutation, which provides an extra positive charge to the H12 helix, also disrupted axonal transport (Figure 6). Previous *in vitro* studies show that the H12 helix supports the motility of KIF5 (Hoenger *et al*, 2000; Uchimura *et al*, 2006) and the microtubule-binding domain of KIF5 is positively charged (Woehlke *et al*, 1997). In this paper, we found that the H12
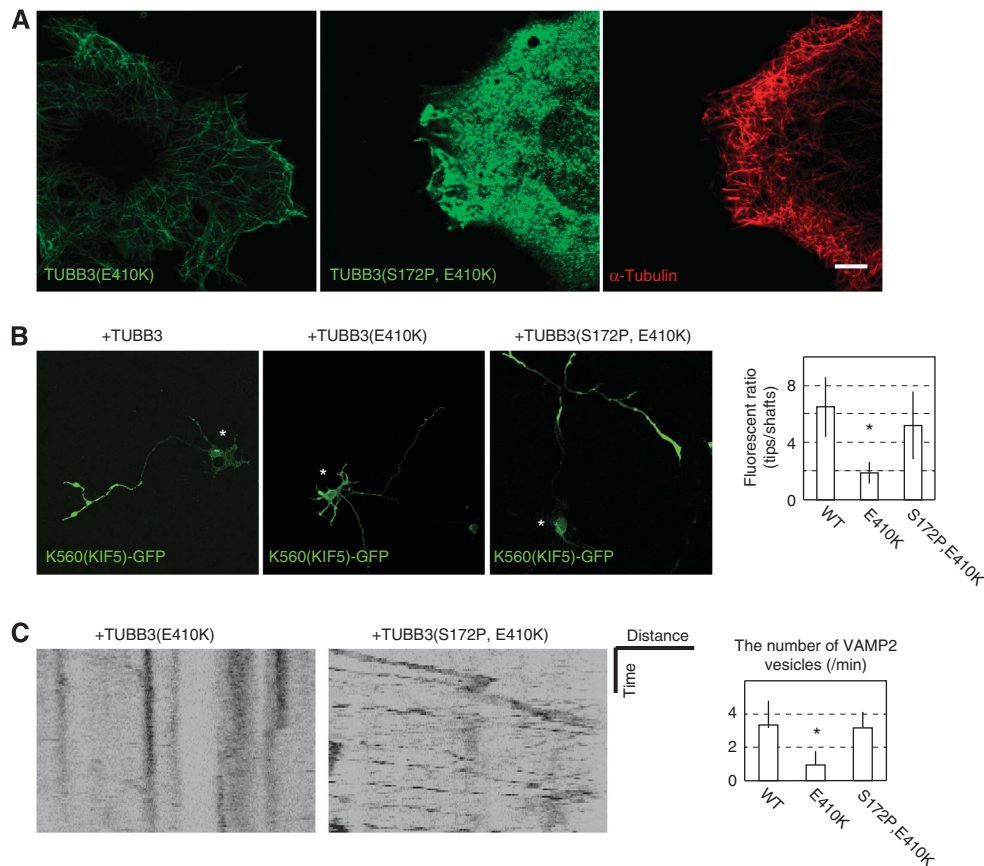
Figure 8 TUBB3(E410K) needs to be incorporated into microtubules to inhibit axonal transport. (**A**) FLAG-TUBB3(E410K) and FLAG-TUBB3(S172P, E410K) vectors were transfected into COS-7 cells, cultured overnight and stained with rabbit anti-FLAG (green) and mouse anti-α-tubulin antibodies (red). Introduction of a S172P mutation makes TUBB3(E410K) cytoplasmic. Bar, 10 μm. (**B**) One microgram of mutant β-tubulin vectors was co-transfected with 2 μg of GFP-K560 vector, incubated for 24 h and observed at 3 div. Representative images are shown. Bar, 50 μm. * indicates cell bodies. Graph shows relative fluorescent intensities calculated by Equation (1). Data are presented as means + s.d. *$P < 0.01$, *t*-test, compared with WT cells. Twenty neurons from three independent transfection were observed in each sample. (**C**) Two micrograms of GFP-VAMP2 and 1 μg of FLAG-β-tubulin-mutant vectors were co-transfected into hippocampal neurons and incubated for 24 h, and live-cell observation was performed. Kymographs indicate the motility of GFP-VAMP2-carrying vesicles in TUBB3(E410K) and TUBB3(S172P, E410K) mutants. The distance and the time scales represent 10 μm and 60 s, respectively. The graph shows the results of quantification. The number of GFP-VAMP2 vesicles moving in axons was counted and is graphically shown. Data are presented as means + s.d. *$P < 0.01$, *t*-test, compared with WT cells. Twenty neurons from three independent transfections were counted.

helix was essential for the axonal tip accumulation of KIFs in neurons (Figures 4–6) and ectopic expression of H12 mutants leads to defective axonal transport and inhibited axon development *in vivo* (Figure 9A–C). While previous studies have analysed the effect of these mutations on mitotic kinesins in yeast cells (Tischfield *et al*, 2010), our results would more clearly and directly suggest the phenomena that cause neuronal symptoms.

Insight into neuronal diseases

Although TUBB3 is a neuron-specific isoform of β-tubulin, only about 20% of total β-tubulin in neuronal cells is TUBB3 (Joshi and Cleveland, 1989). TUBB3(E410K) and TUBB3 (D417H) mutants induce neuronal diseases in an autosomal dominant manner, meaning that only 10% of mutant tubulin can significantly induce neuronal phenotypes. How is this small amount of mutated TUBB3 able to strongly affect neurons? Because our assay used CMV and CAG promoters and unknown copy numbers of transfected vectors, we could not quantify the amount of tubulin incorporated into microtubules in our system. Nevertheless, we think our

results give insights to this question. Microtubules are composed of α- and β-tubulin dimers. The size of each tubulin dimer is 8 nm (Nogales *et al*, 1999). Our analysis showed that TUBB3(E410K) and TUBB3(D417H) were incorporated into microtubules in cells and could inhibit axonal transport (Supplementary Figure S1; Figure 8A). The inhibition of motor domain accumulation, axonal transport and axon development were not observed when the incorporation of mutant tubulin was perturbed by introducing the additional S172P mutation (Figures 8 and 9). Thus, these tubulin mutants need to be co-assembled with normal microtubules to induce neuronal phenotypes. If the 10% mutant TUBB3 is properly incorporated and evenly distributed in neuronal microtubules in CFEOM3 patients, then the distance between TUBB3 mutants is about 80 nm, meaning that KIF-dependent axonal transport is affected every 80 nm (Figure 9D). This distance is short enough to cause an effect because the length of axonal transport is in the order of millimeters to meters (Hirokawa *et al*, 2010). While we hypothesized even distribution of TUBB3 mutant in this model, for more quantitative and precise consideration, the
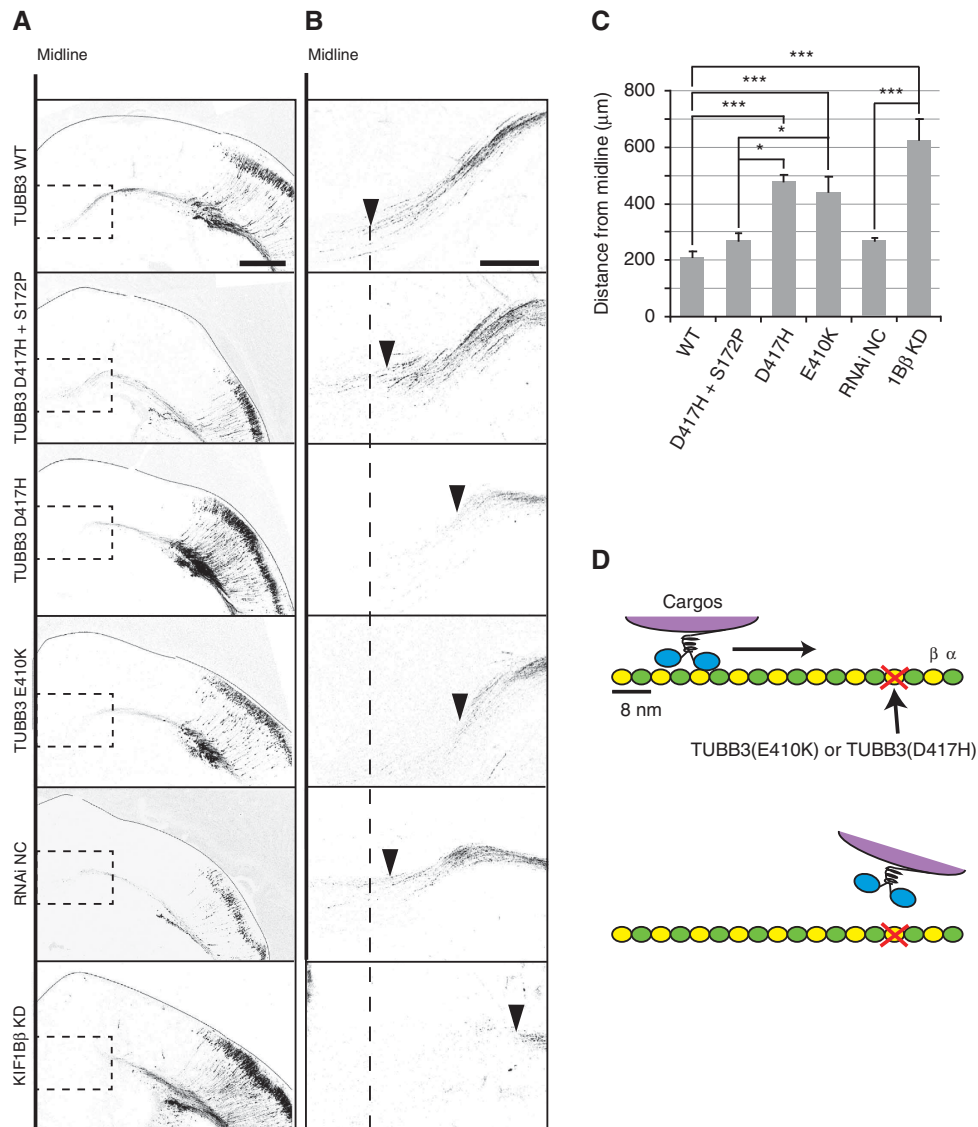
Figure 9 *In utero* electroporation and a model. (**A–C**) TUBB3 mutants or micro RNAs were co-transfected with TurboRFP in E14 embryonic brains and TurboRFP was detected at P1 brains. Fluorescent signals were reversed and shown. Coronal sections of electroporated brains (**A**), and (**B**) high magnification microscopy from (**A**). Arrowheads indicate tips of growing axons. (**C**) Statistical analysis. Distance between the midline and axon tips was measured. $n = 7$ brains for WT, 5 brains for D417H + S172P, 4 brains for D417H, 5 brains for E410K, 3 brains for RNAi Negative Control (NC), 4 brains for KIF1Bβ knockdown from at least two pregnant mice, $*P < 0.05$, $***P < 0.001$, Tukey–Kramer method. Error bars represent s.e.m. Scale bar, 500 μm in (**A**), and 200 μm in (**B**). (**D**) Model of how mutated TUBB3 inhibits KIF-dependent axonal transport. TUBB3(E410K) or TUBB3(D417H) is co-assembled with normal tubulins and dominant negatively inhibit KIF-dependent axonal transport.

developmental change of TUBB3 expression needs to be gauged and it is required to quantify how much amount of mutant tubulin is incorporated into microtubules. It would be helpful to analyse neurons developed from inducible pluripotent stem cells of patients (Abeliovich and Doege, 2009).

Many β-tubulin mutations that cause congenital neuronal diseases have been identified. Depending on the causative mutations, patients who have β-tubulin mutations suffer from various neurological symptoms. In particular, patients with E410K, D417H or D417N mutations suffer from various neurological symptoms, such as loss of axons in the central nervous system, fibrosis of extraocular muscles and peripheral neuropathy, while patients with other mutations do not suffer from these symptoms (Tischfield *et al*, 2010). It has

been suggested that β-tubulin mutations that cause CFEOM3 inhibit the function of KIF21A, because KIF21A mutations cause a similar neuronal disease, CFEOM1 (Yamada *et al*, 2003; Tischfield *et al*, 2010). However, our molecular cell biological analysis of β-tubulin mutants showed that E410K and D417H mutations affect the microtubule binding of not only KIF21A but also of other axonal-transport KIFs (Figure 3). In addition, E410K and D417H β-tubulin mutants disrupt axonal transport of vesicles and mitochondria in cells derived from the central and peripheral nervous systems (Figures 1 and 2). It has been shown that *Kif1a*, *Kif1b* and *Kif5a* mutant mice exhibit divergent neuronal phenotypes, such as loss of axons and peripheral neuropathy-like phenotypes (Yonekawa *et al*, 1998; Zhao *et al*, 2001; Xia *et al*, 2003). Consistent with these previous studies, our

in vivo knockdown of KIF1Bβ induced axonal defects in the brain, the phenotype of which is similar to phenotypes of brains expressing TUBB3(E410K) and TUBB3(D417H) (Figure 9). These phenotypes are similar to symptoms observed in CFEOM3 patients who have TUBB3(E410K) and TUBB3(D417H) mutations (Tischfield *et al*, 2010). In humans, mutations in KIFs induce various neurological diseases (Reid *et al*, 2002; Rivière *et al*, 2011; Klebe *et al*, 2012). Thus, we suggest that the severe symptoms caused by E410K and D417H mutations are because these mutations inhibit not only the function of KIF21A, but also the function of a broad range of axonal transport KIFs in neurons and probably disrupt axonal transport. In contrast, our results show that β-tubulin mutants causing mild CFEOM3 did not significantly affect axonal transport or the localization of KIF21A in cultured neurons (Figures 1–3 and 6). Moreover, the neuronal localization of other KIFs was not affected (Figure 3). Thus, this study has not resolved why other β-tubulin mutations, such as TUBB3(R62Q), cause neuronal phenotypes. It is possible that binding to MAPs and/or microtubule dynamics are changed by these mutations; it has been shown that CFEOM3 mutations change microtubule dynamics in yeast (Tischfield *et al*, 2010). Further study is needed to fully understand the relationship between mutated residues and pathogenesis. A similar cell biological approach to the one we have used, using a different probe such as MAPs or EB3 (Stepanova *et al*, 2003), may facilitate these studies.

Materials and methods

Detailed methods are described in Supplementary data.

Vectors
cDNAs for human KIF21A (KIAA1708) and human KIF1B (KIAA1448) were obtained from the Kazusa DNA Instutute (Chiba, Japan). Mouse TUBB3 (#2700078D11 and #7120476D15), mouse TUBB2 (#6330407N09) and mouse TUBB5 (#I920080M12 and #I730041C01) were obtained from Fantom3 cDNA library (RIKEN, Wako, Japan). C381-GFP and K560-GFP were previously described (Nakata *et al*, 2011; Nakata and Hirokawa, 2003).

Cell culture, transfection and microscopy
Neurons, COS-7 and 293FT cells were cultured as described (Niwa *et al*, 2008). A Ca^{2+}-phosphate transfection kit (TAKARA-Clontech, Tokyo, Japan) was used to transfect hippocampal neurons as described (Jiang and Chen, 2006). One microgram of plasmid DNA was used for a single transfection. For co-transfection, 1 μg of GFP or yellow fluorescent protein (YFP) vector and 2 μg of FLAG-

β-tubulin mutants were used. Co-transfection was checked by immunofluorescence microscopy for each new combination of vectors. For DRG neurons and 293FT cells, electroporation was conducted using a NEON transfection system as described in manufacturer's instructions (Invitrogen). *In utero* electroporation was performed as described (Teng *et al*, 2005). For immunostaining, anti-FLAG (Clone FLG-1; 1:2000 dilution; MBL, Tokyo, Japan), anti-GFP polyclonal (#598; 1:5000 dilution; MBL), anti-tau (Clone tau-1; 1:1000 dilution; Sigma, St Louis, MI, USA) and anti-MAP2 antibodies (Clone HM2; 1:1000 dilution; Sigma) were used. For live-cell imaging, cells were transfected with GFP-VAMP2 (Song *et al*, 2009) and YFP-Rab3A(Q81L) (Niwa *et al*, 2008) as described above. Cells were observed using a LSM710 system (Carl Zeiss, Jena, Germany). For quantification, the pinhole was fully opened and the brightest plane was used. Images were taken by 16-bit mode. To calculate the accumulation of KIFs, the relative fluorescence intensities (Rf) were calculated using the following equation, where S_t, S_s and S_b represent the mean intensity of fluorescence signal in growth cones, axons excluding growth cones and in the background, respectively.

$$Rf = (S_t - S_b)/(S_s - S_b) \tag{1}$$

Microtubule sedimentation
Microtubule binding assays were performed in 293FT cells and brain as described (Bulinski and Borisy, 1979). Anti-Dynein antibodies were described previously (Hirokawa *et al*, 1990).

Structural data
The tubulin structure was processed using UCSF Chimera obtained from the UCSF server (http://www.cgl.ucsf.edu/chimera/). The tubulin structure (Nogales *et al*, 1999) (PDB#1JFF) was obtained from PDB (http://www.pdb.org/pdb/home/home.do).

Supplementary data
Supplementary data are available at *The EMBO Journal* Online (http://www.embojournal.org).

Acknowledgements

Conflict of interest

The authors declare that they have no conflict of interest.

References

Abeliovich A, Doege CA (2009) Reprogramming therapeutics: iPS cell prospects for neurodegenerative disease. *Neuron* **61:** 337–339

Bulinski JC, Borisy GG (1979) Self-assembly of microtubules in extracts of cultured HeLa cells and the identification of HeLa microtubule-associated proteins. *Proc Natl Acad Sci USA* **76:** 293–297

Cleveland DW (1987) The multitubulin hypothesis revisited: what have we learned? *J Cell Biol* **104:** 381–383

Delettre C, Lenaers G, Griffoin JM, Gigarel N, Lorenzo C, Belenguer P, Pelloquin L, Grosgeorge J, Turc-Carel C, Perret E, Astarie-Dequeker C, Lasquellec L, Arnaud B, Ducommun B, Kaplan J, Hamel CP (2000) Nuclear gene OPA1, encoding a mitochondrial dynamin-related protein, is mutated in dominant optic atrophy. *Nat Genet* **26:** 207–210

Hirokawa N (1982) Cross-linker system between neurofilaments, microtubules, and membranous organelles in frog axons revealed by the quick-freeze, deep-etching method. *J Cell Biol* **94:** 129–142

Hirokawa N, Niwa S, Tanaka Y (2010) Molecular motors in neurons: transport mechanisms and roles in brain function, development, and disease. *Neuron* **68:** 610–638

Hirokawa N, Sato-Yoshitake R, Yoshida T, Kawashima T (1990) Brain dynein (MAP1C) localizes on both anterogradely and retrogradely transported membranous organelles in vivo. *J Cell Biol* **111:** 1027–1037

Hoenger A, Thormählen M, Diaz-Avalos R, Doerhoefer M, Goldie KN, Müller J, Mandelkow E (2000) A new look at the microtubule binding patterns of dimeric kinesins. *J Mol Biol* **297:** 1087–1103

Huang CF, Banker G (2011) The translocation selectivity of the kinesins that mediate neuronal organelle transport. *Traffic* **13:** 549–564

Jacobson C, Schnapp B, Banker G (2006) A change in the selective translocation of the Kinesin-1 motor domain marks the initial specification of the axon. *Neuron* 49: 797–804

Jaglin XH, Poirier K, Saillour Y, Buhler E, Tian G, Bahi-Buisson N, Fallet-Bianco C, Phan-Dinh-Tuy F, Kong XP, Bomont P, Castelnau-Ptakhine L, Odent S, Loget P, Kossorotoff M, Snoeck I, Plessis G, Parent P, Beldjord C, Cardoso C, Represa A *et al* (2009) Mutations in the beta-tubulin gene TUBB2B result in asymmetrical polymicrogyria. *Nat Genet* 41: 746–752

Jiang M, Chen G (2006) High Ca2+-phosphate transfection efficiency in low-density neuronal cultures. *Nat Protoc* 1: 695–700

Joshi HC, Cleveland DW (1989) Differential utilization of beta-tubulin isotypes in differentiating neurites. *J Cell Biol* 109: 663–673

Klebe S, Lossos A, Azzedine H, Mundwiller E, Sheffer R, Gaussen M, Marelli C, Nawara M, Carpentier W, Meyer V, Rastetter A, Martin E, Bouteiller D, Orlando L, Gyapay G, El-Hachimi KH, Zimmerman B, Gamliel M, Misk A, Lerer I *et al* (2012) KIF1A missense mutations in SPG30, an autosomal recessive spastic paraplegia: distinct phenotypes according to the nature of the mutations. *Eur J Hum Genet* 20: 645–649

Llopis J, McCaffery JM, Miyawaki A, Farquhar MG, Tsien RY (1998) Measurement of cytosolic, mitochondrial, and Golgi pH in single living cells with green fluorescent proteins. *Proc Natl Acad Sci USA* 95: 6803–6808

Lu S, Zhao C, Zhao K, Li N, Larsson C (2008) Novel and recurrent KIF21A mutations in congenital fibrosis of the extraocular muscles type 1 and 3. *Arch Ophthalmol* 126: 388–394

Mohri H (1968) Amino-acid composition of 'Tubulin' constituting microtubules of sperm flagella. *Nature* 217: 1053–1054

Nakata T, Hirokawa N (1995) Point mutation of adenosine triphosphate-binding motif generated rigor kinesin that selectively blocks anterograde lysosome membrane transport. *J Cell Biol* 131: 1039–1053

Nakata T, Hirokawa N (2003) Microtubules provide directional cues for polarized axonal transport through interaction with kinesin motor head. *J Cell Biol* 162: 1045–1055

Nakata T, Niwa S, Okada Y, Perez F, Hirokawa N (2011) Preferential binding of a kinesin-1 motor to GTP-tubulin-rich microtubules underlies polarized vesicle transport. *J Cell Biol* 194: 245–255

Nangaku M, Sato-Yoshitake R, Okada Y, Noda Y, Takemura R, Yamazaki H, Hirokawa N (1994) KIF1B, a novel microtubule plus end-directed monomeric motor protein for transport of mitochondria. *Cell* 79: 1209–1220

Niwa S, Tanaka Y, Hirokawa N (2008) KIF1B beta- and KIF1A-mediated axonal transport of presynaptic regulator Rab3 occurs in a GTP-dependent manner through DENN/MADD. *Nat Cell Biol* 10: 1269–U1252

Nogales E, Whittaker M, Milligan RA, Downing KH (1999) High-resolution model of the microtubule. *Cell* 96: 79–88

Poirier K, Saillour Y, Bahi-Buisson N, Jaglin XH, Fallet-Bianco C, Nabbout R, Castelnau-Ptakhine L, Roubertie A, Attie-Bitach T, Desguerre I, Genevieve D, Barnerias C, Keren B, Lebrun N, Boddaert N, Encha-Razavi F, Chelly J (2010) Mutations in the neuronal ß-tubulin subunit TUBB3 result in malformation of cortical development and neuronal migration defects. *Hum Mol Genet* 19: 4462–4473

Reid E, Kloos M, Ashley-Koch A, Hughes L, Bevan S, Svenson IK, Graham FL, Gaskell PC, Dearlove A, Pericak-Vance MA, Rubinsztein DC, Marchuk DA (2002) A kinesin heavy chain (KIF5A) mutation in hereditary spastic paraplegia (SPG10). *Am J Hum Genet* 71: 1189–1194

Rivière JB, Ramalingam S, Lavastre V, Shekarabi M, Holbert S, Lafontaine J, Srour M, Merner N, Rochefort D, Hince P, Gaudet R, Mes-Masson AM, Baets J, Houlden H, Brais B, Nicholson GA,

Van Esch H, Nafissi S, De Jonghe P, Reilly MM *et al* (2011) KIF1A, an axonal transporter of synaptic vesicles, is mutated in hereditary sensory and autonomic neuropathy type 2. *Am J Hum Genet* 89: 219–230

Song A, Wang D, Chen G, Li Y, Luo J, Duan S, Poo M (2009) A selective filter for cytoplasmic transport at the axon initial segment. *Cell* 136: 1148–1160

Stepanova T, Slemmer J, Hoogenraad CC, Lansbergen G, Dortland B, De Zeeuw CI, Grosveld F, van Cappellen G, Akhmanova A, Galjart N (2003) Visualization of microtubule growth in cultured neurons via the use of EB3-GFP (end-binding protein 3-green fluorescent protein). *J Neurosci* 23: 2655–2664

Sullivan KF, Cleveland DW (1986) Identification of conserved isotype-defining variable region sequences for four vertebrate beta tubulin polypeptide classes. *Proc Natl Acad Sci USA* 83: 4327–4331

Tanaka Y, Kanai Y, Okada Y, Nonaka S, Takeda S, Harada A, Hirokawa N (1998) Targeted disruption of mouse conventional kinesin heavy chain, kif5B, results in abnormal perinuclear clustering of mitochondria. *Cell* 93: 1147–1158

Teng JL, Rai T, Tanaka Y, Takei Y, Nakata T, Hirasawa M, Kulkarni AB, Hirokawa N (2005) The KIF3 motor transports N-cadherin and organizes the developing neuroepithelium. *Nat Cell Biol* 7: 474–U431

Tischfield MA, Baris HN, Wu C, Rudolph G, Van Maldergem L, He W, Chan WM, Andrews C, Demer JL, Robertson RL, Mackey DA, Ruddle JB, Bird TD, Gottlob I, Pieh C, Traboulsi EI, Pomeroy SL, Hunter DG, Soul JS, Newlin A *et al* (2010) Human TUBB3 mutations perturb microtubule dynamics, kinesin interactions, and axon guidance. *Cell* 140: 74–87

Uchimura S, Oguchi Y, Katsuki M, Usui T, Osada H, Nikawa J, Ishiwata S, Muto E (2006) Identification of a strong binding site for kinesin on the microtubule using mutant analysis of tubulin. *EMBO J* 25: 5932–5941

Verhey K, Hammond J (2009) Traffic control: regulation of kinesin motors. *Nat Rev Mol Cell Biol* 10: 765–777

Woehlke G, Ruby AK, Hart CL, Ly B, Hom-Booher N, Vale RD (1997) Microtubule interaction site of the kinesin motor. *Cell* 90: 207–216

Xia C, Roberts E, Her L, Liu X, Williams D, Cleveland D, Goldstein L (2003) Abnormal neurofilament transport caused by targeted disruption of neuronal kinesin heavy chain KIF5A. *J Cell Biol* 161: 55–66

Yamada K, Andrews C, Chan WM, McKeown CA, Magli A, de Berardinis T, Loewenstein A, Lazar M, O'Keefe M, Letson R, London A, Ruttum M, Matsumoto N, Saito N, Morris L, Del Monte M, Johnson RH, Uyama E, Houtman WA, de Vries B *et al* (2003) Heterozygous mutations of the kinesin KIF21A in congenital fibrosis of the extraocular muscles type 1 (CFEOM1). *Nat Genet* 35: 318–321

Yonekawa Y, Harada A, Okada Y, Funakoshi T, Kanai Y, Takei Y, Terada S, Noda T, Hirokawa N (1998) Defect in synaptic vesicle precursor transport and neuronal cell death in KIF1A motor protein-deficient mice. *J Cell Biol* 141: 431–441

Zhao C, Takita J, Tanaka Y, Setou M, Nakagawa T, Takeda S, Yang HW, Terada S, Nakata T, Takei Y, Saito M, Tsuji S, Hayashi Y, Hirokawa N (2001) Charcot-Marie-Tooth disease type 2A caused by mutation in a microtubule motor KIF1B beta. *Cell* 105: 587–597

Züchner S, Mersiyanova IV, Muglia M, Bissar-Tadmouri N, Rochelle J, Dadali EL, Zappia M, Nelis E, Patitucci A, Senderek J, Parman Y, Evgrafov O, Jonghe PD, Takahashi Y, Tsuji S, Pericak-Vance MA, Quattrone A, Battaloglu E, Polyakov AV, Timmerman V *et al* (2004) Mutations in the mitochondrial GTPase mitofusin 2 cause Charcot-Marie-Tooth neuropathy type 2A. *Nat Genet* 36: 449–451